

This is the preprint of the contribution published as:

Schwenk, C., Negele, S., Balagizi, C.M., Aeschbach, W., **Bohrer, B.** (2022):
High temperature noble gas thermometry in Lake Kivu, East Africa
Sci. Total Environ. **837** , art. 155859

The publisher's version is available at:

<http://dx.doi.org/10.1016/j.scitotenv.2022.155859>

1 **High Temperature Noble Gas Thermometry in Lake**
2 **Kivu**

3 **Cornelis Schwenk^{1,2,6}, Sophie Negele², Charles M. Balagizi^{3,4,5}, Werner**
4 **Aeschbach², and Bertram Boehrer¹**

5 ¹Helmholtz-Centre for Environmental Research – UFZ, Magdeburg - Germany

6 ²Institute of Environmental Physics, Heidelberg University, Heidelberg - Germany

7 ³Geochemistry and Environmental Department, Goma Volcano Observatory, Goma - DR Congo

8 ⁴Department of Chemistry, Institut Supérieur Pédagogique de Bukavu, Bukavu - DR Congo

9 ⁵Istituto Nazionale di Geofisica e Vulcanologia, Sezione di Palermo, Palermo - Italy

⁶ Present address: Institute for Atmospheric Physics, Johannes-Gutenberg University of Mainz

Corresponding author: Cornelis Schwenk, c.schwenk@uni-mainz.de

Abstract

Due to their biological and chemical inertness, noble gases in natural waters are widely used to trace natural waters and to determine ambient temperature conditions during the last intensive contact with the atmosphere (equilibration). Thus far, only common environmental conditions have been considered, and hence investigated temperatures have almost never exceeded 35 °C, but environmental scenarios that generate higher surface-water temperatures (such as volcanism) exist nonetheless. We make use of newly determined solubility data at higher temperatures to analyze data of unexpectedly low noble gas concentrations in the deep water of Lake Kivu by applying various approaches of noble gas thermometry. Noble gas concentration ratios and least squares fitting of individual concentrations indicate that the data agrees best with the assumption that deep water originates from groundwater formed at temperatures of about 65 °C. Thus, no form of degassing is required to explain the observed noble gas depletion: the deep water currently contained in Lake Kivu has most probably never experienced a large scale degassing event. This conclusion is important as limnic eruptions were feared to threaten the lives of the local population.

Keywords: Lake Kivu; Noble gas thermometry; Groundwater formation; Soil temperature; Volcanism; Ebullition.

1 Introduction

Dissolved gases in natural waters are inherited from the atmosphere by equilibrium dissolution and are therefore sensitive to the various conditions of air-water gas exchange. Due to their chemical and biological inertness and their extremely homogeneous composition in the Earth's atmosphere, the noble gases in particular present themselves as ideal geochemical tracers. Measurements of their concentrations have been widely used to reconstruct ambient temperatures during the last intensive contact with the atmosphere (equilibration) (Aeschbach-Hertig & Solomon, 2013; Mazor, 1972; Benson, 1973). This approach, called *noble gas thermometry*, can track groundwater recharge temperatures (Stute et al., 1995; Beyerle et al., 1998; Weyhenmeyer et al., 2000), analyze temperature variations in the past (Stute & Schlosser, 1993; Seltzer et al., 2021) and reconstruct deep ocean recharge temperatures (Loose et al., 2016). Noble gas thermometry has usually focused on equilibration temperatures below 35°C (Aeschbach-Hertig et al., 1999). However, environmental scenarios that generate much higher surface-water temperatures exist (volcanic activity etc.).

41 Lake Kivu, located at the foot of the Nyiragongo volcano, could be such an example
42 of higher temperatures. It contains vast amounts of dissolved carbon dioxide and methane
43 (Tietze et al., 1980; Bärenbold, Schmid, et al., 2020; Boehrer et al., 2019). Most of the
44 CO₂ is of geogenic origin and is brought into the lake by the sub-lacustrine springs and
45 hydrothermal systems (Deuser et al., 1973; Schoell et al., 1988) and by few surface rivers
46 from the Nyamulagira volcanic field (Balagizi et al., 2015). The CH₄ is mainly produced
47 from bacterial reduction of magmatic CO₂ and to a lesser extent from the fermentation of
48 organic material in the sediments. The methane deposit is of great economic value and
49 is being exploited for the production of energy (Boehrer et al., 2019; Schmid et al., 2019;
50 Bärenbold, Boehrer, et al., 2020). The resulting immense gas pressures have been feared to
51 trigger a limnic eruption, as it happened at Lake Nyos and Lake Monoun in Cameroon in
52 1986 and 1984, respectively, and therefore pose a threat to over 2 million local inhabitants
53 of the region (Kusakabe, 2017; Sigurdsson et al., 1987; Kling et al., 1994; Lorke et al.,
54 2004; Boehrer et al., 2021). The recent Nyiragongo volcano eruptions of January 2002 and
55 May 2021 reminded of the precarious situation: magma coming into contact with the deep
56 waters of Lake Kivu could result in local heating and the formation of bubbles which - in the
57 worst case - could trigger a large scale ebullition. In addition, strong earthquakes and large
58 landslides have been listed among external factors that could give rise to a limnic eruption
59 of Lake Kivu, as the lake is located in the floor of a young seismically active rift (Balagizi et
60 al., 2018). The Lake Kivu basin is abound with important tectonic features such as faults,
61 fractures and fissures related to volcanic eruptions and to the rift opening (Balagizi et al.,
62 2016; Pouclet et al., 2016).

63 Recent measurements (Bärenbold, Schmid, et al., 2020) have found unusually low con-
64 centrations of Ne, Ar and Kr in the deep water of Lake Kivu when compared to air-saturated
65 water. At first sight, this could be interpreted as the residual feature of stripped noble gases
66 after a limnic eruption caused by large amounts of escaping methane and carbon dioxide. A
67 closer look revealed that degassing alone could not explain the stronger depletion of heavy
68 noble gases compared to lighter ones (~ 70% for Ar and Kr compared to ~ 45% for Ne).
69 Bärenbold et al. (2020) hence concluded that the groundwater which feeds the lake from
70 below was most probably already depleted of noble gases when it entered the lake.

71 We explore the possibility of higher equilibration temperatures being responsible for
72 the noble gas depletion in Lake Kivu's deep water, as groundwater entering below 260 m is
73 enriched in cations and alkalinity and thus deemed to originate from hydrothermal sources

74 (Ross et al., 2015). We therefore use the extended solubilities of Schwenk et al. (2022) to
 75 make a larger domain of temperatures accessible to noble gas thermometry. We estimate
 76 equilibration temperatures from (1) the saturation concentrations of each noble gas, (2)
 77 ratios of dissolved noble gases and (3) also apply a least squares fitting using the PANGA
 78 software (Jung & Aeschbach, 2018) that allows for excess air formation and an optimized
 79 fit to conclude on the origin of the noble gas deficit.

80 2 Noble Gases in Natural Waters

81 The partial pressure an atmospheric gas i exerts on a water surface can be related to
 82 its water-side concentration in the most common form of Henry's law:

$$p_i = K_{H,i} C_{W,i}, \quad (1)$$

83 where p_i is the partial pressure of a gas i in the atmosphere, $C_{W,i}$ is the concentration of that
 84 gas in water and $K_{H,i}$ is its *Henry coefficient* (Aeschbach-Hertig et al., 1999). Rewriting
 85 Equation 1 in the form:

$$C_{W,i} = L_i \cdot p_i, \quad (2)$$

86 allows us to define the *solubility* $L := 1/K_H$, which describes how much gas is dissolved
 87 in the water phase at a certain partial pressure. If the water-side concentration is given in
 88 $\text{cm}^3\text{STPg}^{-1}$, then the solubility has the units $\text{cm}^3\text{STPg}^{-1}\text{atm}^{-1}$. If equilibration is assumed
 89 to take place at 100% saturation vapor pressure, one can rewrite Equation 2 and explicitly
 90 indicate dependencies on temperature T and altitude z to give:

$$C_{W,i}(T, z) = L_i(T) \cdot (p_{\text{atm}}(z) - e_s(T)) \cdot x_i, \quad (3)$$

91 where $p_{\text{atm}}(z) = p_0 \cdot \exp(-z/H)$ is the total atmospheric pressure at altitude z without regard
 92 to weather variability (and $H = 8700$ m is the scale height assuming a mean temperature
 93 of the relevant air column of 25 °C), $e_s(T)$ is the saturation vapor pressure at temperature
 94 T and x_i is the atmospheric mixing ratio of the gas i . This concentration is also called
 95 the *equilibrium concentration* $C_i^{\text{eq}}(T, p(z))$. When using this formulation it is clear that
 96 the concentration goes to zero at the boiling point, where $e_s(T) = p_{\text{atm}}(z)$. The saturation
 97 vapor pressure required in Equation 3 was calculated using the IAPWS formulation (IAPWS,

1992). Using any form of the Magnus equation would deliver large errors for temperatures above 60 °C (Huang, 2018).

Very few assumptions must be made when using the equilibrium concentration for equilibration temperature reconstruction: calculations of water-side concentrations under various conditions such as different altitudes or no full saturation can be easily applied according to Equation 3. This work utilizes recently published solubilities (Schwenk et al., 2022) that are valid from 0 to 80 °C and are used to depict the equilibrium concentrations of Ne, Ar, Kr and Xe for an altitude of 1460 m (Lake Kivu's surface) in Figure 1.

In groundwater, the concentrations of dissolved noble gases are usually found to be in excess due to the entrapment of air bubbles under higher hydrostatic pressure during formation (Aeschbach–Hertig et al., 2000). The unfractionated air (UA) model describes the complete dissolution of entrapped air bubbles by adding an excess air component A , given in $\text{cm}^3\text{STPg}^{-1}$, multiplied with the atmospheric abundance x_i , to the equilibration concentration C_i^{eq} :

$$C_i(T, p(z), A) = C_i^{eq}(T, p(z)) + Ax_i. \quad (4)$$

This model is the most simple, since it has only three free parameters (two if pressure is assumed) and is therefore the one we applied. More complex models can be found in Aeschbach-Hertig & Solomon (2013).

Natural waters often contain contributions to certain noble gas isotopes that are produced in the subsurface (mainly the Earth's crust) by radioactive decay of parent isotopes (radiogenic), by nuclear reactions (nucleogenic) or as products of nuclear fission (fissiogenic). The most prominent and ubiquitous radiogenic noble gas isotope is ^4He , which is abundantly produced in the decay chains of U and Th present in rocks and minerals. The minor He isotope ^3He often has a nucleogenic contribution, but is also prominently contained in fluids of magmatic (or Earth mantle) origin. Another important radiogenic isotope is ^{40}Ar (from the decay of ^{40}K), which is produced in the crust and also contained in magmatic sources, but usually negligible in shallow groundwaters because of the high atmospheric abundance of Ar. For Ne, the nucleogenic contribution to the rare isotope ^{21}Ne can be relevant in very old groundwaters. Similarly, fissiogenic components of certain Kr and especially Xe isotopes exist, but are usually insignificant in shallow groundwaters.

127 The presence of non-atmospheric noble gas components can be identified through iso-
128 tope ratios that deviate from those in the atmosphere, and when reconstructing equilibration
129 temperatures it is crucial to correct for these contributions, which are not described by the
130 above discussed models (Aeschbach-Hertig & Solomon, 2013). This is possible for Ne and
131 the heavier noble gases by resorting to isotopes of purely atmospheric origin, such as the
132 minor Ar isotope ^{36}Ar . No such isotope exists for He, therefore He is usually not considered
133 in noble gas thermometry.

134 Natural waters can become depleted in noble gases through gas stripping upon bubble
135 formation. This process depletes lighter elements more than heavier elements due to their
136 higher diffusivity (Bourg & Sposito, 2008; Brennwald et al., 2005; Aeschbach-Hertig et al.,
137 2008).

138 2.1 Noble Gas Thermometry

139 In noble gas thermometry one assumes the conditions of groundwater formation (sim-
140 ple, full equilibration according to Equation 3 or more complex models such as the UA
141 model from Equation 4) and infers the temperatures from measurements of noble gas con-
142 centrations. In this work we consider three approaches: noble gas saturation temperatures,
143 noble gas concentration ratio temperatures, and inverse modelling of more complex cases
144 using the PANGA software (Jung & Aeschbach, 2018).

145 The approach of noble gas saturation temperatures assumes simple, full equilibration
146 during groundwater formation. Temperatures T_i^{sat} are thus calculated by numerically invert-
147 ing the equilibrium concentration C_i^{eq} (Equation 3). Uncertainties are determined through
148 the min/max evaluation of temperatures at the upper and lower error bounds of concentra-
149 tion measurements. Figures 1 a) - d) show the equilibrium concentrations evaluated using
150 the recently determined solubilities by Schwenk et al. (2022) from 0 to 80 °C and an altitude
151 of $z = 1460$ m for Ne (a), Ar (b), Kr (c) and Xe (d). We find that the progression is strictly
152 monotonic in all cases, thus allowing for an unambiguous selection of T_i^{sat} .

153 Benson (1973) argued that noble gas concentration ratios can provide a better equi-
154 libration temperature indicator than individual gas concentrations, since effects of pressure,
155 humidity and salinity approximately cancel out (Benson, 1973). The noble gas ratio tem-
156 peratures $T^{\text{NGR}}(i/j)$ can be obtained from measured concentrations $C_{W,i}$ and $C_{W,j}$ of gases

157 i and j by numerically inverting:

$$\frac{C_{W,i}}{C_{W,j}} = \frac{x_i L_i(T)}{x_j L_j(T)}. \quad (5)$$

158 Unlike the saturation temperatures, ratio temperatures do not depend on altitude. The
 159 graphical displays (Figure 1 e) and f)) are thus globally valid. The uncertainties are deter-
 160 mined by evaluating the temperatures at the respective upper/lower and lower/upper error
 161 bounds of concentration measurements. Figure 1 e) shows the Ar to Ne and Figure 1 f) the
 162 Kr to Ne concentration ratios evaluated using solubilities from 0 to 80 °C (Schwenk et al.,
 163 2022). Here we also detect a strictly monotonic progression, which makes the noble gas
 ratio temperature selection unambiguous.

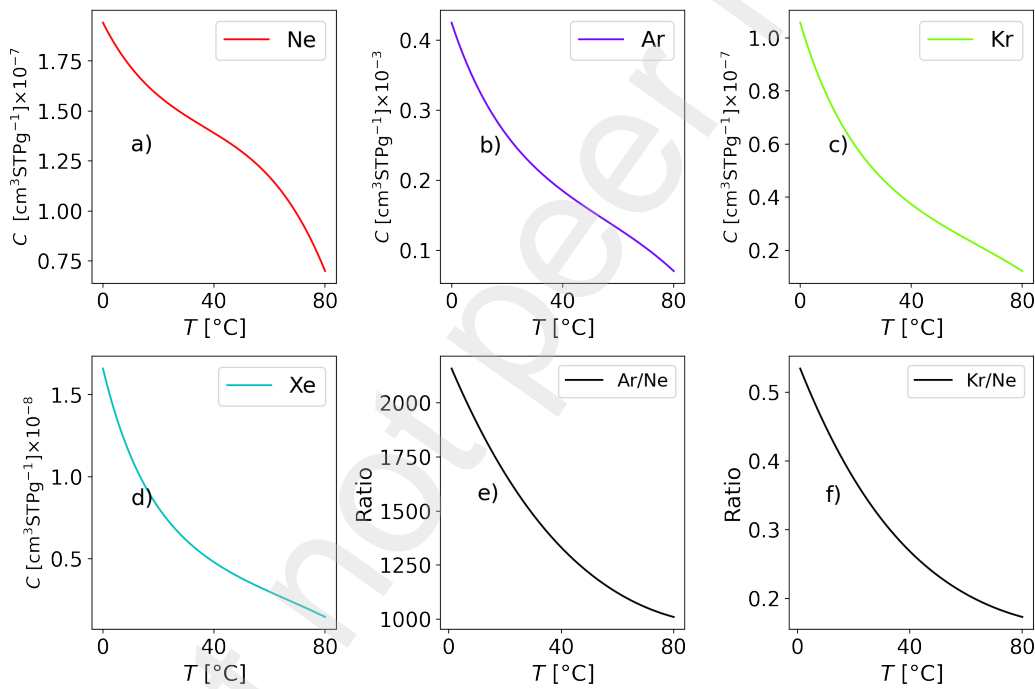


Figure 1. a) - d): Equation 3 evaluated using the newly determined solubilities (Schwenk et al., 2022) from 0 to 80 °C at an altitude of $z = 1460$ m for Ne (a), Ar (b), Kr (c) and Xe (d). The concentration ratios are also evaluated from 0 to 80 °C for Ar to Ne (e) and Kr to Ne (f).

164

165 The PANGA software calculates the UA-model temperatures T^{UA} using the best es-
 166 timates of the different groundwater model parameters through typical methods of in-
 167 verse modeling and simultaneous fitting of multiple noble gas concentrations (Jung &
 168 Aeschbach, 2018). In this work the UA model was applied using the Ne, Ar and Kr con-
 169 centrations with the altitude set to $z = 1460$ m. Concentration measurements C_i^{meas} and

170 the UA-model temperatures were used to calculate the relative excesses/deficits given by
171 $\Delta_i = C_i^{\text{meas}}/C_i^{\text{eq}}(T^{\text{UA}}) - 1$. PANGA delivers uncertainties for the excess air parameter A
172 and the temperature T^{UA} (Jung & Aeschbach, 2018).

173 **3 Lake Kivu**

174 Lake Kivu is a large lake (485 m max depth and 238 km² surface area) located at an
175 altitude of 1460 m in the tectonic and volcanic rift valley of East Africa (Bärenbold, Schmid,
176 et al., 2020; Ross et al., 2015). Within the same rift, the lakes Tanganyika and Malawi are
177 located to the south and Lake Edward and Lake Albert are located to the north. High
178 volcanoes, e.g. Nyiragongo, block the way to the north, and hence the discharge from Lake
179 Kivu flows to the south as the Rusizi River into Lake Tanganyika (Figure 2). Surface inflow
180 happens from small rivers around Lake Kivu, surface run-off and direct precipitation onto
181 the water surface. The location in the tropics at 2 °C south results in two rainy seasons.
182 The lake is meromictic, i.e. the water of the lake is only recirculated to a limited depth
183 during the cool and windy season, leaving the waters below about 80 m depth permanently
184 stratified. The layers below 80 m are entirely deprived of oxygen.

185 Groundwater inflow to the lake is known and has mainly been documented from the
186 north, where active volcanoes dominate the geology (Schmid et al., 2002). The soil in this
187 area originates from acid metamorphic and volcanic parent materials, and is characterized
188 by the presence of thin to large fractures varying from shallow to deep, in addition to
189 fissures acting as high-rate water infiltrating sites. The high water permeability of this soil
190 is responsible for the fact that no surface rivers drain the Nyiragongo volcanic field, whereas
191 only two rivers are found to the extreme south part of Nyamulagira volcano, both discharging
192 into Kabuno bay (Balagizi et al., 2015). In this area, three main groundwater recharge
193 zones are identified based on stable isotopes from precipitation, rivers and springs: the
194 lower altitude recharge zone ranging from altitudes of ~ 1800 to 2150 m asl, an intermediate
195 zone ranging from ~ 2180 to 2500 m, and the third zone located at higher altitudes ranging
196 from ~ 2620 to 3220 m (Balagizi et al., 2022). In the lake, two depth horizons are known
197 for the inflow of groundwater into the deep waters: warm subaquatic groundwater discharge
198 (SGD) (of higher density due to elevated salinity and high content of carbon dioxide and
199 methane) entering between maximum depth and 450 m and a strong input at around 260 m
200 depth of cool and fresh SGD (Ross et al., 2015). This results in a temperature profile that
201 increases from 23 °C in the upper layer to 26 °C in the lower layer (see Figure 3), while

202 electrical conductivity rises from roughly 2 mS/cm to 5 mS/cm. The surplus of groundwater
 203 causes a slow vertical upwelling of water masses. Waters in the deepest layers are enriched
 204 in cations and alkalinity and therefore all deemed to originate from hydrothermal sources,
 205 while the upper layers consist of a mixture of volcanic and fresher groundwater (Ross et al.,
 206 2015; Bärenbold et al., 2022). The increased temperature of the deep SGDs is hypothesized
 to originate from a deep magma reservoir existing below Lake Kivu.

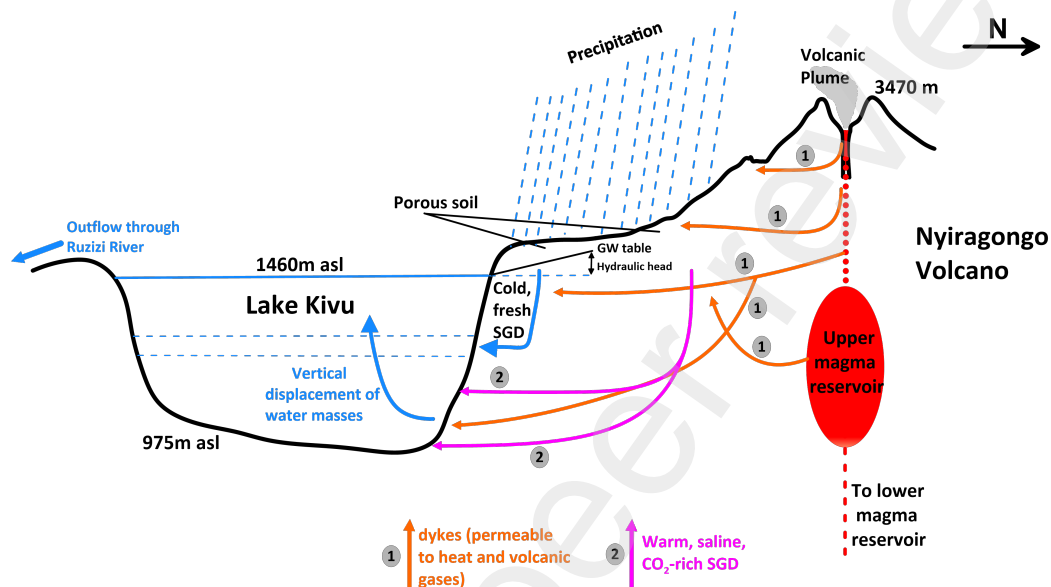


Figure 2. Sketch (not to scale) of the location and the hydrological situation of Lake Kivu within the East African Rift Valley. From the Nyiragongo magma reservoir, heat and volcanic gases could be injected through permeable fractures (proposed by Ross et al., 2015 and Balagizi et al., 2016) and could possibly heat groundwater before it is completely sealed off from the atmosphere, thus allowing for an equilibration at high temperatures. Some of these fractures extend beneath Lake Kivu (Villeneuve, 1980; Wauthier et al., 2012; Balagizi et al., 2018).

207

3.1 Noble Gases in Lake Kivu

208

209 Bärenbold et al. (2020) provide a comprehensive dataset of noble gas concentrations and
 210 isotopic ratios in Lake Kivu. Their findings, depicted in Figures 3 e) to f), defy expectations:
 211 noble gases (Ne, Ar, Kr) are strongly depleted in the deep waters of Lake Kivu with respect
 212 to air saturated water (ASW) at the conditions of the lake surface (1460 m, 25 °C). Ne
 213 is depleted by $\sim 45\%$ and the more soluble heavy noble gases Ar (^{36}Ar) and krypton by
 214 $\sim 70\%$. Xe measurements show peculiar variabilities and were therefore discarded by the
 215 authors. He concentrations and the $^{40}\text{Ar}/^{36}\text{Ar}$ ratio increase with depth and thus deliver
 216 strong evidence for the existence of magmatic sources. The $^{20}\text{Ne}/^{22}\text{Ne}$ ratio is constant

217 at the atmospheric value (Bärenbold, Schmid, et al., 2020). These results are extremely
 218 curious since groundwater almost always shows excess air components that lead to higher
 concentrations contrary to the observations in Lake Kivu.

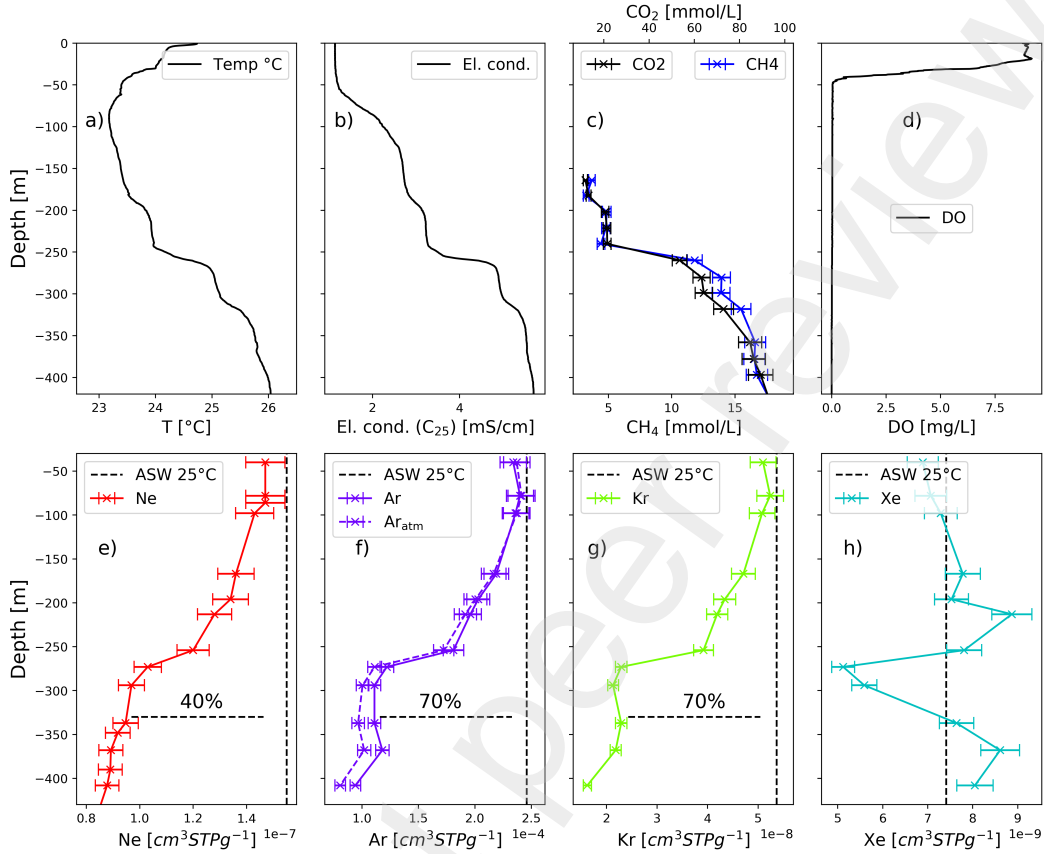


Figure 3. Vertical profiles in Lake Kivu: a) Temperature, b) electrical conductivity normalized to 25 °C, c) dissolved CH₄ and CO₂ and d) dissolved oxygen (Boehrer et al., 2019). The increasing salinity and CO₂ allow for stability of the stratification even though the temperature increases with depth. e) - h) show the noble gas concentrations (Bärenbold, Schmid, et al., 2020), whereby in f) the total Ar and the corrected atmospheric Ar (dashed lines, see Equation 6) are shown. Black dashed lines in e) - h) show concentrations obtained through equilibration at 25 °C and Lake Kivu's altitude, called air saturated water (ASW).

219

220 Bärenbold et al. (2020) ruled out two possible explanations of the noble gas deficits
 221 in the deep water: continuous outgassing by bubble-stripping should lead to kinetic frac-
 222 tionation of the ²⁰Ne/²²Ne ratio and also should affect Ne more strongly than Ar and Kr;
 223 a large scale limnic eruption in the past was deemed implausible since after a general gas
 224 depletion the lowest layers of the lake, which are replenished by the subaquatic groundwater
 225 inflows, should be the first to return to saturation, in contrast to observations. The authors
 226 conclude that the most realistic scenario is hydrothermal groundwater being heated in the

227 volcanic subsoil and partitioning with a gas or steam phase, thereby losing noble gases and
 228 entering the deep water already depleted. One issue with this scenario however, as stated
 229 by the authors, is that one would expect a larger depletion in Ne than in Ar and Kr due
 230 to the lower solubility of lighter noble gases. Instead of contact with steam they therefore
 231 suggest that hydrothermal groundwater either exchanges noble gases with an oil phase or
 232 that large amounts of excess air occurred during groundwater formation, which could have
 233 enriched Ne in the initial groundwater. We instead propose and investigate whether the
 234 depletion can be explained by higher temperatures during groundwater formation.

235 He has significant sources and hence was not included in further considerations; nor
 236 did we use Xe, as it showed such inconsistencies that Bärenbold et al. (2020) discarded it.
 237 Since ^{40}Ar can have magmatic sources and the $^{40}\text{Ar}/^{36}\text{Ar}$ ratio in the deep water is up to
 238 20% higher than the atmospheric value we calculated the atmospheric Ar using ^{36}Ar :

$$C(\text{Ar}_{\text{atm}}) = C(^{36}\text{Ar}) / 0.003336. \quad (6)$$

239 $C(\text{Ar}_{\text{meas}}) - C(\text{Ar}_{\text{atm}})$ equals the magmatic ^{40}Ar and it correlates to the measured ^3He con-
 240 centration with a linear correlation coefficient of $R^2 = 0.96$, showing that this is a good
 241 correction.

242 4 Results

243 The noble gas saturation temperatures T_i^{sat} are presented in Figure 4 a) for Ne (red),
 244 Ar (purple), atmospheric Ar (purple dashed line) and Kr (green) under the assumption
 245 of an equilibration altitude of $z = 1460$ m (Lake Kivu's surface altitude). The measured
 246 in-situ temperature is also shown (black). In the upper 100 m, the noble gas saturation
 247 temperatures correspond to the measured in situ-temperature. This is expected, since the
 248 upper layers mix annually and thus equilibrate with the atmosphere. Below 260 m, the
 249 depth at which measured noble gas concentrations decrease dramatically, temperatures of
 250 60 to 65 °C (Kr, Ar) and 70 to 75 °C (Ne, Ar_{atm}) are found.

251 The noble gas ratio temperatures are depicted in Figure 4 b). In the upper layers
 252 all noble gas ratio temperatures lie at ~ 25 °C and below ~ 260 m they all show a sharp
 253 increase to higher temperatures. The Ar to Ne temperature that corrects for contributions
 254 of magmatic Ar (dashed purple line) delivers higher temperatures than the other ratio
 255 temperatures throughout the lower layers.

256 In the T^{UA} evaluation the excess air variable A is included in the optimization proce-
 257 dure. The temperatures T^{UA} , excess air parameters A and the relative excesses/deficits Δ_i
 258 are depicted in Figure 4b) - d). PANGA delivers temperatures of $\sim 25^\circ\text{C}$ for the upper
 259 layers, $\sim (65 \pm 2)^\circ\text{C}$ for the lower layers below 260 m, and $\sim (75 \pm 2)^\circ\text{C}$ for the deepest
 260 measurement. The excess air parameter A fluctuates around a small negative value not far
 261 from zero within the error bounds. A negative value for A indicates undersaturation but
 262 is not physical because it corresponds to simply removing a certain amount of atmospheric
 263 air from the water, for which no known process exists. However, negative values of A could
 264 be due to either degassing or equilibration at a lower atmospheric pressure, i.e., a higher
 altitude.

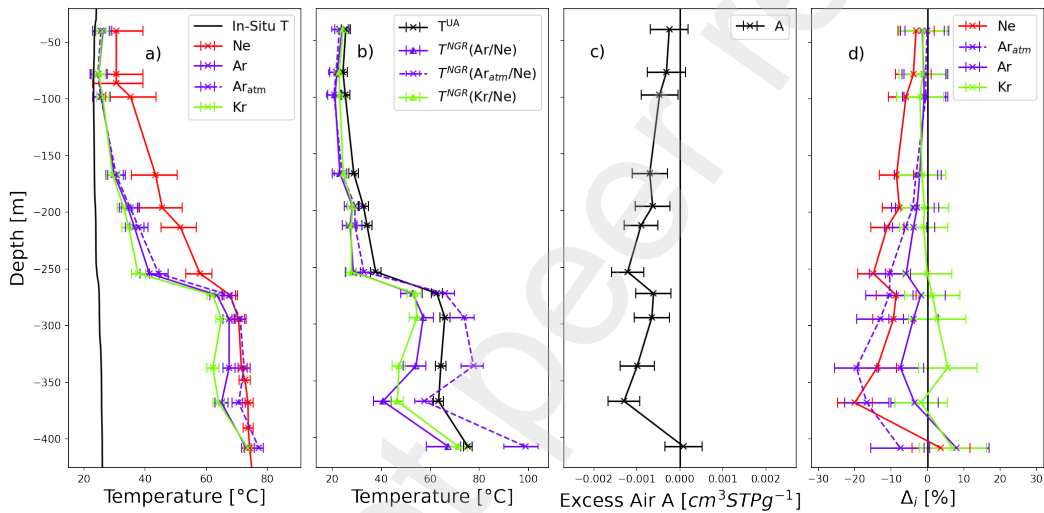


Figure 4. Results: a) The measured in-situ temperature (black) and the noble gas saturation temperatures T_i^{sat} obtained for Ne (red), Ar (purple), atmospheric Ar (purple dashed) and Kr (green) under the assumption of an equilibration altitude of $z = 1460$ m (lake level). b) - d) Optimization results from PANGA and temperatures derived from Kr/Ne and $\text{Ar}_{\text{atm}}/\text{Ne}$ ratios for Lake Kivu, assuming equilibration at lake level and unfractionated excess air (UA-model): b) noble gas temperatures against depth. c) unfractionated excess air parameter (deficit for negative value) d) relative excess/deficit Δ_i against depth.

265

266 By setting the equilibration altitude to ~ 2200 m, an altitude that not only provides a
 267 sufficient hydraulic head for the water to enter the lake, but is also easily reached by the
 268 intermediate groundwater recharge zone around the Nyiragongo volcano that ranges from \sim
 269 2180 to 2500 m, one obtains values for A that instead fluctuate around zero and the resulting
 270 temperatures remain close to unchanged. When applying this altitude the values for Δ_i also
 271 shift closer to zero in the deeper layers. It is thus possible to explain the observed noble gas

272 concentrations through the single mechanism of a high temperature equilibration at a high
 273 altitude.

274 Xe measurements were discarded by the authors of Bärenbold et al. (2020) since they
 275 showed a puzzling structure. Using the UA-model temperatures, the theoretically expected
 276 concentration of Xe was calculated and the difference to the actual Xe concentration inter-
 277 preted as a theoretical "excess Xe" (Figure 5). Excess Xe is positive over the entire water
 278 column, indicating the presence of a possible source. In addition, we find a correlation of
 279 excess Xe with magmatically attributed ^3He and excess ^{40}Ar ($R^2 \sim 0.92$).

280 Noticeable concentrations of fissiogenic xenon have so far however only been found in
 281 waters that are many millions of years old, owing to the very small subsurface production
 282 rates of Xe isotopes (Lippmann et al., 2003). The travel time of the groundwater that
 283 discharges into the deep parts of Lake Kivu is unknown but is constrained by the fact
 284 that the current hydrogeologic situation in the Virunga volcanic Province at the northern
 285 shore of Lake Kivu only evolved in the late Pleistocene and the Holocene. The activity
 286 of the volcanoes Nyiragongo and Nyamulagira began 14 - 10 kyr ago, which led to the
 287 closure of the lake's outflow to the north and consequently a strong lake level rise and the
 288 start of subaquatic volcanism (Ross et al., 2014). The possibility of finding a strong xenon
 289 component of magmatic or fissiogenic origin in the lake or the surrounding groundwater
 290 could therefore constitute an exciting finding.

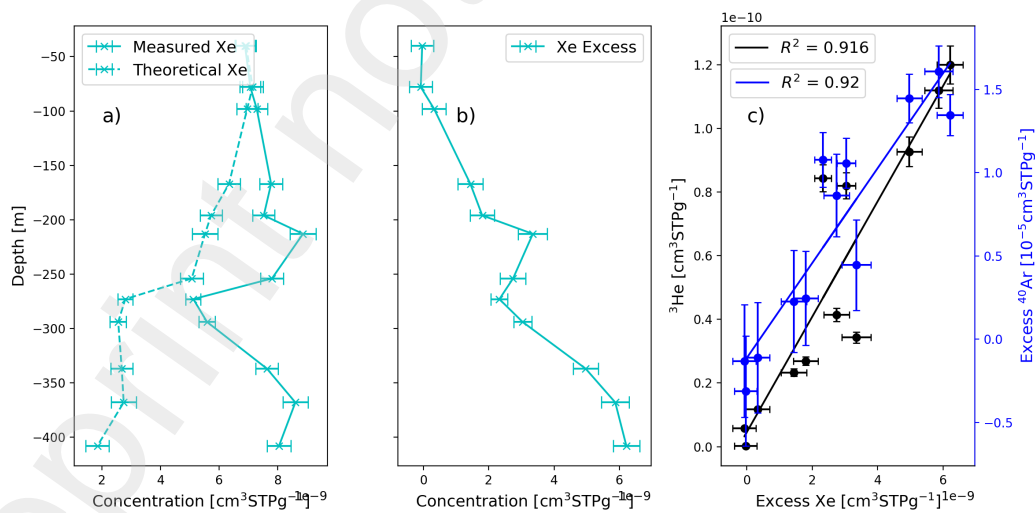


Figure 5. Excess Xe: a) Measured Xe concentrations in Lake Kivu (solid line) and theoretically expected Xe (dashed line). b) Theoretical excess Xe profile. c) Correlation of measured ^3He (black) and calculated excess ^{40}Ar (blue) to the theoretical excess Xe.

5 Conclusions

This is the first study to implement noble gas thermometry at high temperatures and the first to apply it to lakes. We used the new solubility functions from Schwenk et al. (2022) to analyze measurements made by Bärenbold et al. (2020) in Lake Kivu where the deep water is dominated by groundwater inflow. The results indicate that the observed noble gas deficits can entirely be explained through groundwater formation at high temperatures. For the upper layers, i.e., as far as seasonal recirculation operates, our approach delivered the expected temperatures of 25 °C. We discovered that for an equilibration altitude of some hundred meters above Lake Kivu's surface level, groundwater formation temperatures for the deep layers below 260 m of (65 ± 2) °C and for the deepest measurement a temperature of (75 ± 2) °C can entirely explain the observed noble gas concentrations in Lake Kivu.

Our findings are in contrast to earlier investigations (Mazor, 1972), which had found that hydrothermal waters had been equilibrated at atmospheric temperatures and pressures and heated only later, at larger depth. We do not challenge this general understanding of hydrothermal water formation. However, noble gas concentrations indicate equilibration at higher temperatures in the Lake Kivu area and this could also be the case in other volcanic locations. The inferred case of air equilibration under hydrothermal conditions followed by cooling in the subsurface requires an extension of the usual range of NGT determination.

Most importantly for the local population, however, the missing noble gases in Lake Kivu can be explained by equilibration at higher temperatures and hence are not indicative of catastrophic ebullition events. Lowering the gas pressure in Lake Kivu's deep water would however still contribute to safety and must be continued with the necessary caution.

6 Outlook

Our approach of noble gas thermometry can be applied to other cases where groundwater formation could take place at higher temperatures. In addition, a search for high groundwater temperatures close to the surface in areas around the Nyiragongo volcano may be stimulated by our results. In addition, more measurements of noble gases in Lake Kivu, especially of Xe, if possible of multiple isotopes, would better constrain fits and factors such as gases of volcanic origin. One could also make use of the high-temperature solubility functions from Schwenk et al. (2022) to create a high-temperature subsurface equilibration model that might even better explain the noble gas signatures.

322 **Acknowledgments**

323 CS did the numerical calculations and was the primary author. SN updated the PANGA
324 software for our purposes. CMB provided geological expertise. WA contributed his expertise
325 on noble gas thermometry. BB developed the idea of the study and provided expertise. All
326 authors contributed to the writing and all authors participated in the whole process of this
327 study.

References

- 328
- 329 Aeschbach-Hertig, W., El-Gamal, H., Wieser, M., & Palcsu, L. (2008). Modeling excess air
330 and degassing in groundwater by equilibrium partitioning with a gas phase. *Water*
331 *Resources Research*, *44*, W08449. doi: 10.1029/2007WR006454
- 332 Aeschbach-Hertig, W., Peeters, F., Beyerle, U., & Kipfer, R. (1999). Interpretation of
333 dissolved atmospheric noble gases in natural waters. *Water Resources Research*, *35*(9),
334 2779-2792. doi: <https://doi.org/10.1029/1999WR900130>
- 335 Aeschbach-Hertig, W., & Solomon, D. K. (2013). Noble gas thermometry in groundwater
336 hydrology. In P. Burnard (Ed.), *The noble gases as geochemical tracers* (pp. 81–122).
337 Springer.
- 338 Aeschbach-Hertig, W., Peeters, F. J. C., Beyerle, U., & Kipfer, R. (2000). Palaeotemperature
339 reconstruction from noble gases in ground water taking into account equilibration
340 with entrapped air. *Nature*, *405*, 1040-1044.
- 341 Balagizi, C. M., Darchambeau, F., Bouillon, S., Yalire, M. M., Lambert, T., & Borges, A. V.
342 (2015). River geochemistry, chemical weathering, and atmospheric CO₂ consumption
343 rates in the Virunga volcanic province (East Africa). *Geochem. Geophys. Geosyst.*,
344 *16*(8), 2637–2660.
- 345 Balagizi, C. M., Kasereka, M., A.M., K., Cuoco, E., Arienzo, I., & Marcello, L. (2022).
346 Characterizing groundwater recharge sources using water stable isotopes in the north
347 basin of Lake Kivu, East Africa. *under review - chemical geology*.
- 348 Balagizi, C. M., Kies, A., Kasereka, M. M., Tedesco, D., Yalire, M. M., & McCausland,
349 W. A. (2018). Natural hazards in Goma and the surrounding villages, East African
350 rift system. *Nat. Hazards (Dordr.)*, *93*(1), 31–66.
- 351 Balagizi, C. M., Yalire, M. M., Ciraba, H. M., Kajeje, V. B., Minani, A. S., Kinja, A. B.,
352 & Kasereka, M. M. (2016). Soil temperature and CO₂ degassing, SO₂ fluxes and
353 field observations before and after the February 29, 2016 new vent inside Nyiragongo
354 crater. *Bull. Volcanol.*, *78*(9).
- 355 Bärenbold, F., Boehrer, B., Grilli, R., Mugisha, A., von Tümpling, W., Umutoni, A., &
356 Schmid, M. (2020). No increasing risk of a limnic eruption at Lake Kivu: Intercom-
357 parison study reveals gas concentrations close to steady state. *PLoS One*, *15*(8), 1–14.
358 doi: 10.1371/journal.pone.0237836
- 359 Bärenbold, F., Kipfer, R., & Schmid, M. (2022). Dynamic modelling provides new insights
360 into development and maintenance of Lake Kivu's density stratification. *Environ.*

- 361 *Model. Softw.*, 147(105251), 105251.
- 362 Bärenbold, F., Schmid, M., Brennwald, M. S., & Kipfer, R. (2020). Missing atmospheric
363 noble gases in a large, tropical lake: The case of Lake Kivu, East-Africa. *Chemical*
364 *Geology*, 532, 119374. doi: 10.1016/j.chemgeo.2019.119374
- 365 Benson, B. (1973). Noble gas concentration ratios as paleotemperature indicators. *Geochim.*
366 *Cosmochim. Acta*, 37, 1391–1395.
- 367 Beyerle, Purtschert, Aeschbach-Hertig, Imboden, Loosli, Wieler, & Kipfer. (1998). Climate
368 and groundwater recharge during the last glaciation in an ice-covered region. *Science*
369 *(New York, N.Y.)*, 282(5389), 731–734. doi: 10.1126/science.282.5389.731
- 370 Boehrer, B., Saiki, K., Ohba, T., Tanyileke, G., Rouwet, D., & Kusakabe, M. (2021).
371 Carbon dioxide in lake Nyos, Cameroon, estimated quantitatively from sound speed
372 measurements. *Front. Earth Sci.*, 9.
- 373 Boehrer, B., Tümpling, W., Mugisha, A., Rogemont, C., & Umutoni, A. (2019). Reliable
374 reference for the methane concentrations in Lake Kivu at the beginning of industrial
375 exploitation. *Hydrology and Earth System Sciences*, 23, 4707–4716.
- 376 Bourg, I. C., & Sposito, G. (2008). Isotopic fractionation of noble gases by diffusion in
377 liquid water: Molecular dynamics simulations and hydrologic applications. *Geochim.*
378 *Cosmochim. Acta*, 72, 2237–2247.
- 379 Brennwald, M., Kipfer, R., & Imboden, D. (2005). Release of gas bubbles from lake sediment
380 traced by noble gas isotopes in the sediment pore water. *Earth and Planetary Science*
381 *Letters*, 235(1-2), 31–44. doi: 10.1016/j.epsl.2005.03.004
- 382 Deuser, W. G., Degens, E. T., Harvey, G. R., & Rubin, M. (1973). Methane in Lake Kivu:
383 new data bearing on its origin. *Science*, 181(4094), 51–54.
- 384 Huang, J. (2018). A simple accurate formula for calculating saturation vapor pressure of
385 water and ice. *Journal of Applied Meteorology and Climatology*, 57(6), 1265–1272.
386 doi: 10.1175/JAMC-D-17-0334.1
- 387 IAPWS. (1992). Revised supplementary release on saturation properties of ordinary wa-
388 ter substance. (SRI-86). Retrieved from [http://www.iapws.org/relguide/Supp-sat](http://www.iapws.org/relguide/Supp-sat.pdf)
389 [.pdf](http://www.iapws.org/relguide/Supp-sat.pdf)
- 390 Jung, M., & Aeschbach, W. (2018). A new software tool for the analysis of noble gas data
391 sets from (ground)water. *Environmental Modelling & Software*, 103, 120–130. doi:
392 10.1016/j.envsoft.2018.02.004
- 393 Kling, G. W., Evans, W. C., Tuttle, M. L., & Tanyileke, G. (1994). Degassing of Lake Nyos.

- 394 *Nature*, 368(6470), 405–406. doi: 10.1038/368405a0
- 395 Kusakabe, M. (2017). Lakes Nyos and Monoun gas disasters (Cameroon)—limnic eruptions
396 caused by excessive accumulation of magmatic CO₂ in crater lakes. *Geochemistry*
397 *Monograph Series*, 1(1), 1–50. doi: 10.5047/gems.2017.00101.0001
- 398 Lippmann, J., Stute, M., Torgersen, T., Moser, D. P., Hall, J. A., Lin, L., ... Onstott,
399 T. C. (2003). Dating ultra-deep mine waters with noble gases and ³⁶Cl, Witwatersrand
400 Basin, South Africa. *Geochim. Cosmochim. Acta*, 67(23), 4597–4619. doi: 10.1016/
401 S0016-7037(03)00414-9
- 402 Loose, B., Jenkins, W. J., Moriarty, R., Brown, P., Jullion, L., Naveira Garabato, A. C., ...
403 Meredith, M. P. (2016). Estimating the recharge properties of the deep ocean using
404 noble gases and helium isotopes. *Journal of Geophysical Research: Oceans*, 121(8),
405 5959–5979. doi: 10.1002/2016JC011809
- 406 Lorke, A., Tietze, K., Halbwachs, M., & Wüest, A. (2004). Response of lake Kivu strat-
407 ification to lava inflow and climate warming. *Limnology and Oceanography*, 49(3),
408 778–783. doi: 10.4319/lo.2004.49.3.0778
- 409 Mazor, E. (1972). Paleotemperatures and other hydrological parameters deduced from gases
410 dissolved in groundwaters, Jordan Rift Valley, Israel. *Geochim. Cosmochim. Acta*, 36,
411 1321–1336.
- 412 Pouclet, A., Bellon, H., & Bram, K. (2016). The cenozoic volcanism in the Kivu rift:
413 Assessment of the tectonic setting, geochemistry, and geochronology of the volcanic
414 activity in the South-Kivu and Virunga regions. *Journal of African Earth Sciences*,
415 121, 219–246.
- 416 Ross, K. A., Gashugi, E., Gafasi, A., Wüest, A., & Schmid, M. (2015). Characterisation
417 of the subaquatic groundwater discharge that maintains the permanent stratification
418 within lake Kivu; East Africa. *PloS one*, 10(3), e0121217. doi: 10.1371/journal.pone
419 .0121217
- 420 Ross, K. A., Smets, B., de Batist, M. A., Hilbe, M., Schmid, M., & Anselmetti, F. S.
421 (2014). Lake-level rise in the late pleistocene and active subaquatic volcanism since
422 the Holocene in Lake Kivu; East African Rift. *Geomorphology*, 221, 274–285.
- 423 Schmid, M., Bärenbold, F., Boehrer, B., Darchambeau, F., Grilli, R., Triest, J., & Tümpling,
424 W. (2019). Intercalibration campaign for gas concentration measurements in Lake
425 Kivu..
- 426 Schmid, M., Tietze, K., Halbwachs, M., Lorke, A., McGinnis, D. F., & Wüest, A. (2002).

- 427 How hazardous is the gas accumulation in lake Kivu? arguments for a risk assesment
428 in light of the Nyiragongo volcano eruption of 2002. *Acta Vulcanologica*, 14/15(1-2),
429 115–122.
- 430 Schoell, M., Tietze, K., & Schoberth, S. M. (1988). Origin of methane in Lake Kivu
431 (East-Central Africa). *Chem. Geol.*, 71(1-3), 257–265.
- 432 Schwenk, C., Negele, S., Aeschbach, W., & Boehrer, B. (2022). Extending noble gas solu-
433 bilities in water to higher temperatures for environmental application. *under review -*
434 *ACS journal of chemical and engineering data*.
- 435 Seltzer, A. M., Ng, J., Aeschbach, W., Kipfer, R., Kulongoski, J. T., Severinghaus, J. P.,
436 & Stute, M. (2021). Widespread six degrees Celsius cooling on land during the Last
437 Glacial Maximum. *Nature*, 593(7858), 228–232. doi: 10.1038/s41586-021-03467-6
- 438 Sigurdsson, H., Devine, J. D., Tchia, F. M., Presser, F. M., Pringle, M., & Evans, W. C.
439 (1987). Origin of the lethal gas burst from Lake Monoun, Cameroon. *Journal of*
440 *Volcanology and Geothermal Research*, 31(1-2), 1–16. doi: 10.1016/0377-0273(87)
441 90002-3
- 442 Stute, M., Forster, M., Frischkorn, H., Serejo, A., Clark, J. F., Schlosser, P., . . . Bonani, G.
443 (1995). Cooling of tropical brazil (5°C) during the Last Glacial Maximum. *Science*,
444 269(5222), 379–383.
- 445 Stute, M., & Schlosser, P. (1993). Principles and applications of the noble gas paleother-
446 mometer. In P. K. Swart, K. C. Lohmann, J. Mckenzie, & S. Savin (Eds.), *Climate*
447 *change in continental isotopic records* (pp. 89–100). Washington, D. C.: American
448 Geophysical Union. doi: 10.1029/GM078p0089
- 449 Tietze, K., Geyh, M., Müller, H., Schröder, L., Stahl, W., & Wehner, H. (1980). The
450 genesis of the methane in Lake Kivu (Central Africa). *Geologische Rundschau*, 69(2),
451 452–472. doi: 10.1007/BF02104549
- 452 Villeneuve, M. (1980). La structure du rift Africain dans la région du Lac Kivu (Zaire
453 oriental). *Bull. Volcanol.*, 43(3), 541–551.
- 454 Wauthier, C., Cayol, V., Kervyn, F., & d'Oreye, N. (2012). Magma sources involved in
455 the 2002 Nyiragongo eruption, as inferred from an InSAR analysis. *J. Geophys. Res.*,
456 117(B5).
- 457 Weyhenmeyer, Burns, Waber, Aeschbach-Hertig, Kipfer, Loosli, & Matter. (2000). Cool
458 glacial temperatures and changes in moisture source recorded in Oman groundwaters.
459 *Science (New York, N. Y.)*, 287(5454), 842–845. doi: 10.1126/science.287.5454.842